Nanostructured Semiconductor Composites for Solar Cells

Review of Fundamentals, Characterization Tools, and Related Composites

by Vaidyanathan (Ravi) Subramanian

Extensive use of non-renewable fossil fuels for conventional energy production is depleting global reserves rapidly. Further, greenhouse gas emissions, increasing production costs of non-renewable fossil fuels, and unreliable geopolitical constraints have underscored the need to develop alternate energy sources. One area that is continuing to attract a lot of interest is the possibility of energy generation from the sun. The focus of solar energy utilization has mainly been toward electricity (photovoltaics[1]) and hydrogen (water splitting[2,3]) generation. Photovoltaic systems absorb energy from sunlight to produce electricity.[4-6] Photovoltaic systems are a promising alternative source of energy because they produce electricity directly from light in one step with none of the problems that one otherwise faces with other sources of energy. Photovoltaic cells have proven applications in distributed power, satellite systems, and portable devices.[7]

Operating Principle of a Liquid-Junction Photovoltaic Cell

Figure 1 shows a schematic of a liquid junction-based photovoltaic cell. It consists of a photo*anode*, a counter electrode *cathode*, and a *reference* electrode. The photoanode absorbs energy (hν) when it is exposed to solar radiation to create electrons (e^-) and holes (h^+). The photogenerated electrons are driven to an underlying conducting substrate either naturally or by the application of an external bias voltage to generate a *photocurrent*. At the same instant, photogenerated holes are scavenged by the surrounding electrolyte and carried to the cathode where they recombine with the electrons and complete the circuit. Voltage and the current flow are typically expressed with respect to a reference electrode.

The effectiveness of such a photovoltaic cell in converting solar energy to electricity depends upon several factors. Some of these are the efficiency with which light is absorbed by the photoanode, the number of e^- - h^+ pairs generated at the photoanode (which depends on the incident photon flux), and the stability of the photoanode. By this account, the photoanode can be considered as a vital component that affects the cell performance. The properties of the materials that are used in the preparation of the photoanode can have a major influence in the overall operational efficiency of the cell. A majority of the research effort is therefore focused on developing novel materials for photoanodes.

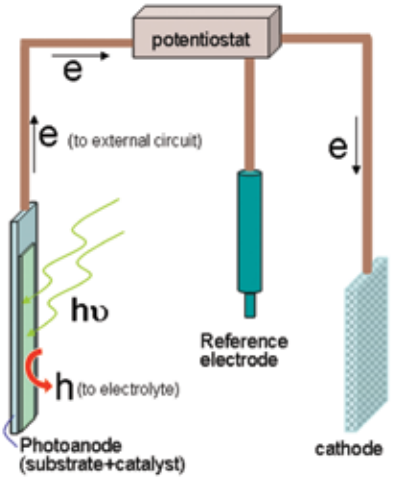

Fig. 1. *Scheme illustrating the process of solar-to-electric conversion.*

An ideal photoanode should

- absorb light from a substantial part of the solar spectrum efficiently,
- offer high surface area (to absorb maximum light),
- effectively utilize the absorbed energy to produce maximum electron-hole pairs,
- facilitate rapid transport of the charges,
- be inexpensive and easily available,
- be non-corrosive and non-toxic, and
- be stable in the electrolyte for a long time.

Inorganic Semiconductors as Solar Harvesting Materials

Semiconductor oxides,[5,8] organic,[9] and polymer-based composites[9,10] are examples of some of the materials proposed as possible candidates for photoanodes. Among these, inorganic semiconductor oxides have attracted considerable interest since they satisfy several of the aforementioned requirements.

In an ideal defect-free semiconductor, electrons are distributed in such a way that they occupy energy levels in a completely filled band (called the *valence band*-VB) which is separated from a higher-lying empty band (called the *conduction band*-CB). The gap between these two bands is called *bandgap* (E_g).[11] Depending upon the size of the gap, a semiconductor can absorb light from any portion of the solar spectrum. One can manipulate the bandgap by simply changing the particle size of the semiconductor. This process is called *size quantization effect* (Fig. 2) and is observed in several inorganic semiconductor oxides.[12,13] The effects of quantization can be monitored using photoelectrochemical techniques.[14]

Atomic vacancies can create irregularities (called *defects*) in the lattice structure of the inorganic semiconductor. The defects are represented as energy states (referred to as *trap sites*) within the bandgap. The defects also alter the electronic properties of the semiconductor to make it an n-type or p-type semiconductor. Under photo illumination, e^- - h^+ pairs generated in the semiconductor can be localized at the electron (e_t) and hole (h_t) trap sites. The traps will delay or prevent the electrons from moving to the external

circuit. These e^- - h^+ pairs can also undergo recombination resulting in a decrease in photocurrent generation (the dotted lines in the nanoparticle shown in Fig. 2 represent possible routes for e^- - h^+ recombination). Thus, defects can play a vital role in controlling the photoelectrochemical activity of a semiconductor.[15,16]

In addition to the above issues, contact of a semiconductor with an electrolyte can result in the formation of an electrical double layer that causes the deformation of the bandgap at the semiconductor surface. The direction of this deformation depends upon the nature of defects (n-or p-type). This process is called band bending. Figure 2 shows the band bending in an n-type semiconductor. The extent of band bending depends on many factors (applied potential, semiconductor doping level, etc.) and influences e^- - h^+ pair separation. An application of external voltage can change the extent of band bending.[3] The sign and magnitude of the external voltage can be manipulated up to a point where the bands can flatten and cause the current direction to reverse. Control of charge flow in the case of nanoparticulate films is also achieved by application of suitable bias voltage.[11]

Electrochemical Characterization Methods

I-V and I-t measurements. Standardized electrochemical methods are employed to measure the photoelectrochemical performance.[17,18] These include current (I)–voltage (V) and current–time(t) plots that indicate the photoelectrochemical activity of different photoanode materials for solar-to-electric conversion. Reconstructed profiles of responses to photoillumination of an n-type semiconductor photoanode are shown in Fig. 3. Figure 3a shows an I-V plot along with schematic illustrations explaining the response in different sections of the plot. The application of a positive bias (for an n-type semiconductor) to the illuminated film facilitates the flow of the photogenerated electrons to the external circuit (*anodic current*). A negative external bias opposes the flow of photogenerated electrons and reduces the magnitude of the anodic current until it reaches a point where no current flows through the circuit. A further application of negative bias results in a reversal in the current flow. The point where this current reversal takes place is called the *flat-band potential*. The location of the flat-band potential can provide a preliminary estimate of the extent of charge separation and voltage difference

(continued on next page)

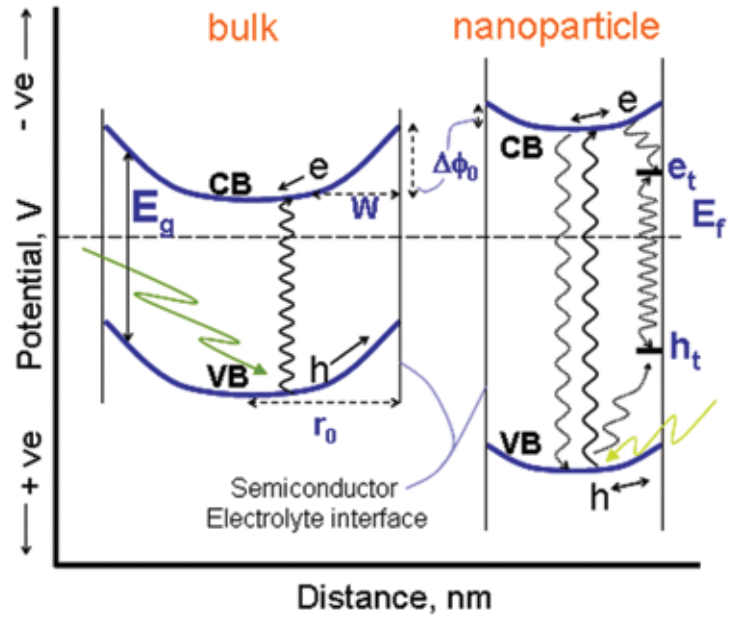

$$\Delta\phi = \left(\frac{kT}{6e}\right)\left(\frac{r-(r_0-W)}{L_D}\right)\left(1+\frac{2(r_0-W)}{r}\right)$$

$\Delta\phi$ = *potential difference*
κ = *Boltzmann constant*
r_0= *radius of the particle*
W= *width of the depletion layer*
L_D = *Debye length*

Fig. 2. *Energy diagram of a semiconductor bulk and nanoparticle showing physical changes (quantization effect) and details of various electronic processes that occur under illumination.*

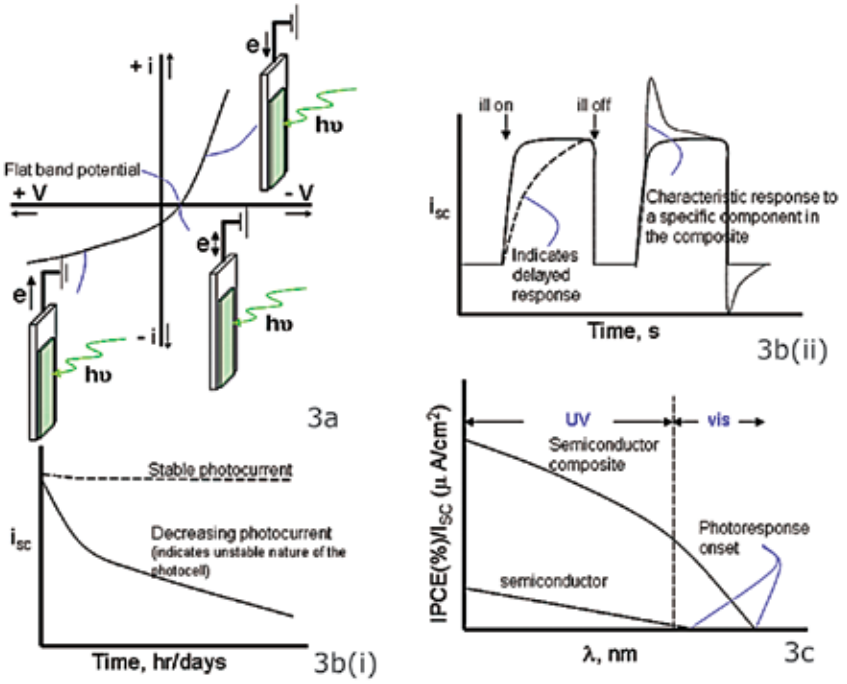

Fig. 3. *Reconstructed profiles of responses to illumination of an n-type semiconductor photoanode in a solar cell. (a) An I-V curve (the location of flat-band potential indicates the extent of charge separation at the photoanode). (b) An I-t plot that demonstrates the stability of the photoanode under (i) long-term continuous and (ii) short-term discontinuous illumination of the solar cell. (c) The response characteristics (IPCE or action spectrum) of the photoanode.*

Table I. Other parameters to evaluate solar cell performance.

Parameters	Representation	Significance
Incident light intensity	I_L [25,26]	The relationship between this parameter and short circuit current (I_{sc}) is often used to correlate how many photons contribute to electron generation and to assess carrier recombination and charge-transfer kinetics losses.
Open-circuit potential	V_{oc} [25]	This parameter is a measure of how efficient the charge separation is in a given semiconductor-liquid combination.
Power	$P = I_{sc} * V_{oc}$ [27]	It is an estimate of how much power can be drawn from the solar cell. P_{max} is the maximum power output.
Fill factor	$P_{max}/V_{oc} * I_{sc}$ [27]	It is a lumped parameter that indicates how well the system is operating. This estimate includes contributions such as the light absorption efficiency and the number of electrons generated and transported across the film.

that can be developed following illumination of the photoanode.

Fig. 3b(i) shows chronoamperometry data under continuous[18,19] and discontinuous [20] illumination. Monitoring the photocurrent during continuous illumination can reveal information about the stability of the photoanode. Several factors can cause a decrease in the photocurrent under long-term illumination. One reason could be a reversible or an irreversible chemical transformation at the photoanode.[21] Analysis of the results from periodic discontinuous illumination can provide information about the transient behavior of photoandes.[22-24]

Figure 3b(ii) shows a few examples of the responses observed when a photoanode is illuminated periodically. The shape of the transients obtained from discontinuous illumination can assist in identifying the source that contributes to limiting the flow of charges. Some of the factors that can contribute to a delayed response (shown as a dashed and dotted lines in Fig. 3b(ii)) are electrolyte concentration, magnitude of applied potential, illumination intensity, thickness of the photoanode film, and/or surface area of the photoanode. Table I lists several other variables that assist in the evaluation of the photoanode properties.

Charge separation efficiency. Effectiveness of charge separation is an important criterion for identifying a promising material for a photoanode.[5,20,28] The most common method for measuring the effectiveness of charge separation is to calculate the *incident photon to current conversion efficiency (IPCE)*. It is calculated by using the following expression:

$$\text{IPCE}\ (\%) = \frac{1240 \times I_{sc}\,(A/cm^2)}{\lambda\,(nm) \times I_{inc}\,(W/cm^2)} \times 100 \qquad (1)$$

where I_{SC} = short circuit current, I_{inc} = incident light power.

Figure 4 shows the derivation of this equation. Figure 3c shows a typical IPCE plot (photoaction spectrum). In a generic sense, this plot can also be interpreted as a measure of how many electrons are generated in the external circuit for every 100 photons that are incident on the photoanode. One can also identify the contribution of each wavelength of incident light to electron flow to the external circuit. Furthermore, if the photoanode is a composite, the onset of the plot response is compared with the absorbance spectra of the photoanode film to identify the specific materials of the composite that contributes to absorbing light from different sections of the incident beam.[29]

Semiconductor-based Composite Materials as Photoanodes

One of the most popular and extensively investigated semiconductors for application as photoanodes in a solar cell is titanium dioxide (TiO_2). TiO_2 has a bandgap of ~3.2 eV (VB edge = -0.5 V and

$$\textit{Quantum yield}\ (\phi) = \frac{\textit{number of charge carriers}\ (n)}{\textit{number of photons}\ (N)}$$

$$\textit{multiply and divide by}\ e/s\ \textit{to estimate current per unit area}$$

$$(\phi) = \frac{en/s}{eN/s} = \frac{I_{SC}\,(amp/cm^2)}{eN/s\,/cm^2} \qquad (i)$$

$$\textit{Total incident power}\ (P)\ \textit{in}\ watt/cm^2\ \textit{is given as}$$

$$P = Nh\upsilon = Nh\frac{c}{\lambda}$$

$$N = \frac{P\lambda}{hc} \qquad (ii)$$

$$\textit{substituting (ii) in (i)}$$

$$(\phi) = \frac{I_{SC}hc}{eP\lambda} = \frac{I_{SC}(amp/cm^2) \times 6.62\times10^{-34}\,Js \times 3\times10^{8}\,m/s}{1.6\times10^{-19}\,coulombs \times P(watt/cm^2) \times \lambda(nm) \times 10^{-9}\,m}$$

$$IPCE(\phi)\% = \frac{1240 \times I_{SC}\,(amp/cm^2)}{P(watt/cm^2) \times \lambda(nm)}$$

Fig. 4. *Derivation of the expression for the IPCE parameter.*

Table II. Examples of semiconductor based photoanode composites.

Composite materials	Example	IPCE	Application	Ref.
Semiconductor and metal	TiO_2 TiO_2 –Au TiO_2 –Pt	5% 28% 27%	Minimize charge recombination, improve photocurrent.	18
Semiconductor and dye	TiO_2 TiO_2– Ru based dye	60% 80%	Dye improves the ability of the photoanode to absorb light from visible and IR regions.	30
Semiconductor with another semiconductor	TiO_2 TiO_2-CdSe	5% 16%	Depending upon the particle size of the CdSe component, different sections of visible light can be absorbed.	31
Doped semiconductor and dye	TiO_2 N-doped TiO_2 N-doped TiO_2 -Ru-CBB[a]	28% 14% 28%	While the TiO_2 alone is not photoactive in the visible, the addition of dye to the doped TiO_2 makes it photoactive in the visible.	32

[a] Ru-CBB: cisdithiocyanato-bis(2,2′-bipyridyl-4,4′-dicarboxylate)-ruthenium (II)

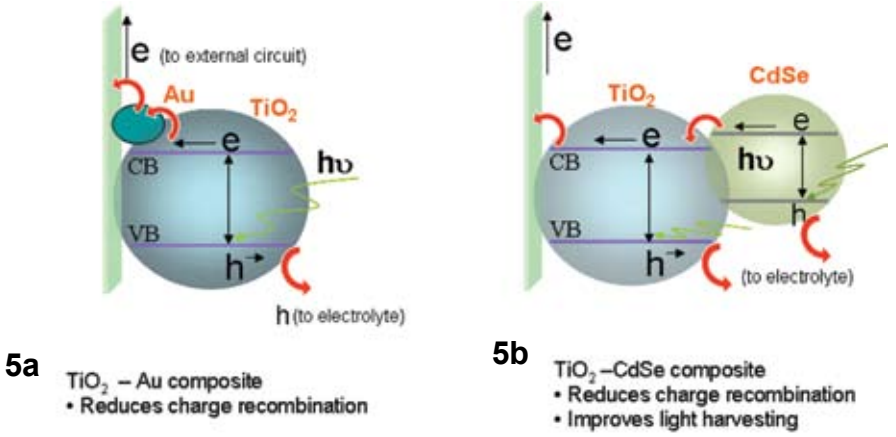

Fig. 5. *(a) The steps involved in the transport of photogenerated electrons from the semiconductor to the substrate via gold nanoparticles. Favorable energetics are essential for charge transport. (b) The scheme to improve the solar to electric conversion using CdSe deposited over TiO_2.*

CB edge = -2.7 V vs. the standard hydrogen reference), which makes it photoactive in the UV portion of the solar spectrum. However, the UV portion of the solar spectrum accounts for just ~3% of the total energy radiated by the sun. In order to make the photovoltaic cell efficient, there are three directions that researchers are currently pursuing: improve photocurrent generation by minimizing charge recombination across the bandgap; develop materials that can absorb light from visible and IR portions of the light spectrum; and develop materials that satisfy both the criteria listed above.

A few examples of semiconductor based composites are shown in Table II. The IPCE values from Table II indicate that composites in general are observed to outperform semiconductors. The mechanism of charge generation, separation, and path of transport for representative composites belonging to some of the categories listed in Table II is shown schematically in Fig. 5. For example, a metal can be deposited over a semiconductor to synthesize a composite that improves charge separation by decreasing recombination. Figure 5a shows the mechanism of charge transfer from a TiO_2 conduction band to the collecting substrate via a gold nanoparticle. It is possible to employ this method to decrease recombination in a semiconductor because metals function as sinks for photogenerated electrons. Another approach is to deposit a second semiconductor over the TiO_2. Cadmium selenide (CdSe) is a small bandgap (E_g ~1.6-2.7 eV versus SHE) semiconductor that absorbs visible light to generate e-h pairs. The bandgaps of CdSe and TiO_2 are located such that photogenerated electrons from the CB of CdSe are injected into the CB of TiO_2 and collected at the substrate as shown in Fig. 5b. The advantage of this scheme is that both TiO_2 and CdSe can absorb light from different portions of the solar spectrum and thus improve the overall efficiency of the solar-to-electric conversion process.

Conclusions

Semiconductor based composite materials for solar photovoltaic conversion has evolved into a mature field thanks to the research by several groups around the globe. The approaches discussed here for improving solar-to-electric conversion are promising but have to be further developed before they are practically useful. For example, sensitization into the visible range may come at a cost in the form of loss in the absorption capability of the photoanode in the UV portion of the spectrum.[32] Improvement in charge separation using metal nanoparticles can bring instability during long-term illumination.[18] Clearly, while several options are available, there is still room for improvement.

Review articles on the current status of photovoltaics, opportunities, and other issues are available.[7,33,34] Readers are further referred to authoritative articles related to specific topics such as dye sensitized solar cells,[35] metal–semiconductor composites,[36] and organic semiconductors.[34] Conversion of solar energy using photovoltaics is emerging as a serious technology option to satisfy our energy requirements. Considering the growth of this area and in the context of our present energy needs, it can be expected to be a major player in alternate energy solutions for the foreseeable future.

Acknowledgments

The work discussed in this article has been performed by the author as a part of the PhD thesis at Notre Dame Radiation Laboratory under the guidance of Professors Prashant Kamat and Eduardo Wolf. Funding from the Department of Energy, the University of Nevada, Reno College

(continued on next page)

of Engineering, and Office of the Vice President for Research is greatly appreciated.

■

References

1. K. Kalyanasundaram and M. Grätzel, *P. Indian Acad. of Sci.-Chem. Sci.,* **109**, 447 (1997).
2. A. Fujishima and K. Honda, *Nature,* **49**, 37 (1972).
3. T. Bak, J. Nowotny, M. Rekas, and C. C. Sorrell, *Int. J. Hydrogen Energ.,* **27**, 991 (2002).
4. M. Fischer, *Int. J. Hydrogen Energ.,* **11**, 495 (1986).
5. M. Grätzel, *Nature,* **414**, 338 (2001).
6. M. Grätzel, *Coord. Chem. Rev.,* **111**, 167 (1991).
7. R. W. Miles, *Vacuum,* **80**, 1090 (2006).
8. G. K. Mor, O. K. Varghese, M. Paulose, K. Shankar, and C. A. Grimes, *Sol. Ener. Mat. Sol. C,* **90**, 2011 (2006).
9. G. A. Chamberlain, *Sol. Cells,* **8**, 47 (1983).
10. X. Y. Deng, L. P. Zheng, C. H. Yang, Y. F. Li, G. Yu, and Y. Cao, *J. Phys. Chem. B,* **108**, 3451 (2004).
11. J. Singh, *Semiconductor Devices: An Introduction,* 2nd ed.; McGraw-Hill Companies (1994).
12. K. F. Lin, H. M. Cheng, H. C. Hsu, L. J. Lin, and W. F. Hsieh, *Chem. Phys. Lett.,* **409**, 208 (2005).
13. Z. A. Peng and X. G. Peng, *J. Am. Chem. Soc.,* **123**, 183 (2001).
14. T. Torimoto, S. Nagakubo, M. Nishizawa, and H. Yoneyama, *Langmuir,* **14**, 7077 (1998).
15. D. S. Zhang, J. A. Downing, F. J. Knorr, and J. L. McHale, *J. Phys. Chem. B,* **110**, 21890 (2006).
16. Y. Hamasaki, S. Ohkubo, K. Murakami, H. Sei, and G. Nogami, *J. Electrochem. Soc.,* **141**, 660 (1994).
17. N. Chandrasekharan and P. V. Kamat, *J. Phys. Chem. B,* **104**, 10851 (2000).
18. V. Subramanian, E. E. Wolf, and P. V. Kamat, *J. Phys. Chem. B,* **105**, 11439 (2001).
19. K. Sayama, S. Tsukagoshi, K. Hara, Y. Ohga, A. Shinpou, Y. Abe, S. Suga, and H. Arakawa, *J. Phys. Chem. B,* **106**, 1363 (2002).
20. C. Nasr, P. V. Kamat, and S. Hotchandani, *J. Phys. Chem. B,* **102**, 10047 (1998).
21. V. Subramanian, E. E. Wolf, and P. V. Kamat, *Langmuir,* **19**, 469 (2003).
22. N. R. de Tacconi, M. Mrkic, and K. Rajeshwar, *Langmuir,* **16**, 8426 (2000).
23. N. R. de Tacconi, C. A. Boyles, and K. Rajeshwar, *Langmuir,* **16**, 5665 (2000).
24. S. G. Hickey, D. J. Riley, and E. J. Tull, *J. Phys. Chem. B,* **104**, 7623 (2000).
25. C. Nasr, S. Hotchandani, P. V. Kamat, S. Das, K. G. Thomas, and M. V. George, *Langmuir,* **11**, 1777 (1995).
26. C. Santato, M. Ulmann, and J. Augustynski, *J. Phys. Chem. B,* **105**, 936 (2001).
27. I. Bedja, S. Hotchandani, and P. V. Kamat, *J. Phys. Chem.,* **98**, 4133 (1994).
28. Y. Diamant, S. G. Chen, O. Melamed, and A. Zaban, *J. Phys. Chem. B,* **107**, 1977 (2003).
29. N. J. Cherepy, G. P. Smestad, M. Grätzel, and J. Z. Zhang, *J. Phys. Chem. B,* **101**, 9342 (1997).
30. M. K. Nazeeruddin, P. Pechy, T. Renouard, S. M. Zakeeruddin, R. Humphry-Baker, P. Comte, P. Liska, L. Cevey, E. Costa, V. Shklover, L. Spiccia, G. B. Deacon, C. A. Bignozzi, and M. Grätzel, *J. Am. Chem. Soc.,* **123**, 1613 (2001).
31. I. Robel, V. Subramanian, M. K. Kuno, and P. V. Kamat, *J. Am. Chem. Soc.,* **128**, 2385 (2006).
32. T. Lindgren, J. M. Mwabora, E. Avendano, J. Jonsson, A. Hoel, C. G. Granqvist, and S. E. Lindquist, *J. Phys. Chem. B,* **107**, 5709 (2003).
33. M. G. Thomas, H. N. Post, and R. DeBlasio, *Prog. Photovoltaics,* **7**, 1 (1999).
34. M. Grätzel, *MRS Bull.,* **30**, 23 (2005).
35. K. Kalyanasundaram and M. Grätzel, *Coord. Chem. Rev.,* **177**, 347 (1998).
36. P. V. Kamat, *Pure Appl. Chem.,* **74**, 1693 (2002).

About the Author

Vaidyanathan (Ravi) Subramanian is an assistant professor of chemical and metallurgical engineering at the University of Nevada at Reno. His current research interests include the development of nancomposite materials for application as photoanodes in solar cells, catalysts for fuel cells, and catalyst-support composites for high temperature renewable hydrocarbon reforming to produce hydrogen. He may be reached at ravisv@unr.edu.